Journal of Hazardous Materials 182 (2010) 97–107

Contents lists available at ScienceDirect

Journal of Hazardous Materials

journal homepage: www.elsevier.com/locate/jhazmat

Characteristics of organosulphur compounds adsorption onto Jordanian zeolitic tuff from diesel fuel

Faisal Mustafa[a], Mohammad A. Al-Ghouti[b,*], Fawwaz I. Khalili[a], Yahya S. Al-Degs[c]

[a] Department of Chemistry, University of Jordan, Amman 1194, Jordan
[b] Royal Scientific Society, Industrial Chemistry Centre, P.O. Box 1438, Al-Jubiha, Amman 11941, Jordan
[c] Department of Chemistry, Hashemite University, Zarqa, Jordan

ARTICLE INFO

Article history:
Received 21 January 2010
Received in revised form 31 May 2010
Accepted 1 June 2010
Available online 8 June 2010

Keywords:
Diesel fuel
Organosulphur compounds
Zeolitic tuff
Adsorption

ABSTRACT

The removal of organosulphur compounds (ORS) from diesel fuel is an important aspect of Jordanian's effort to reduce air pollution. Currently, the total sulphur content in Jordanian diesel fuel is 12000 ppmw (1.2%, wt/wt), but Jordanian government has recently introduced new restrictions that will reduce this level gradually to internationally acceptable levels. The zeolitic tuff (ZT), from Tlul Al-Shahba region, was characterised using various analytical techniques. It was found that the Freundlich model fitted the adsorption isotherms more accurately than the Langmuir model; indicating that the ZT had a heterogeneous surface. The Langmuir adsorption capacity values for the three particle size ranges (100–200), (300–400), and (500–600) μm were 7.15, 6.32, and 5.52 mg/g and the column capacities were 4.45, 2.57, and 1.92 mg/g, respectively. The spent ZT was regenerated by washing with n-heptane with an efficiency of 81.5%. Two adsorption mechanisms were investigated. One is that the interaction of thiophene with the Brønsted site of the ZT through S atoms; the other is via C–S bond cleavage in thiophene-derived carbocations to form unsaturated fragments on the Brønsted acid sites.

1. Introduction

Organosulphur compounds (ORS) in fuels cause toxic emissions and inefficient performance of exhaust catalysts; thus, processes for their removal have been widely explored [1]. The ORS are usually present in almost all fractions of crude oil distillation [2,3]. The low boiling crude oil fractions contain mainly the aliphatic organosulphur compounds and the higher boiling crude oil fractions above 250 °C predominantly contain thiophenic rings as shown in Fig. 1.

Thiophene, benzothiophene, and their alkyl derivatives are the most abundant ORS in diesel fuel; more reactive sulphides, disulphides, and mercaptans are present as minor components. Thiophene represents a particular challenge, because they resemble abundant arenes and alkenes in electron density and basicity; thus making chemical specificity difficult during adsorption and catalysis. The high specific area, the surface functional groups, the structural, and compositional flexibility make zeolite (ZT) a potential candidate for thiophene adsorption [2,3].

Due to the increasingly stringent environmental regulations on the sulphur content in transportation fuels, desulphurisation of diesel fuel has become a very important research topic. The ORS are the main cause of acid rain and poisoning of catalysts in CO and NO_x catalytic converters [4]. The ORS in diesel fuel have a detrimental effect on the performance of catalysts used in vehicle and have environmental problems. It is generally agreed that the sulphur content in hydrocarbon fuels has to be reduced to less than 35–350 parts per million by weight for vehicle applications. Currently, the total sulphur content in Jordanian diesel oil is 12000 ppmw (1.2%, wt/wt). Therefore, there is a dire need to incorporate desulphurisation technologies into the fuel processor.

The ORS are known to be slightly polar than hydrocarbons of similar nature. The exploitation of the polarity factor has been the subject of numerous investigations for processes based on oxidation/extraction and adsorption [2,3]. A typical adsorption process is expected to offer selective removal of ORS, to operate at normal temperature and pressure with ease of operation/ease of process control and economically achieve near total elimination of ORS from transportation fuels. At the same time, ease of regeneration with minimum requirement of chemical and energy is also expected from the point of view of commercial viability. A wide variety of materials starting from activated carbon (AC), silica-based sorbents, zeolites, and metal exchanged/impregnated AC/zeolites/mesoporous materials have been reported in the past for adsorption [5].

Naturally Jordanian occurring zeolites are supposed to be good candidates to be manipulated as solid adsorbents because of their

* Corresponding author.
E-mail addresses: mghouti@rss.gov.jo, ghoutijo@yahoo.co.uk (M.A. Al-Ghouti).

0304-3894/$ – see front matter © 2010 Elsevier B.V. All rights reserved.
doi:10.1016/j.jhazmat.2010.06.003

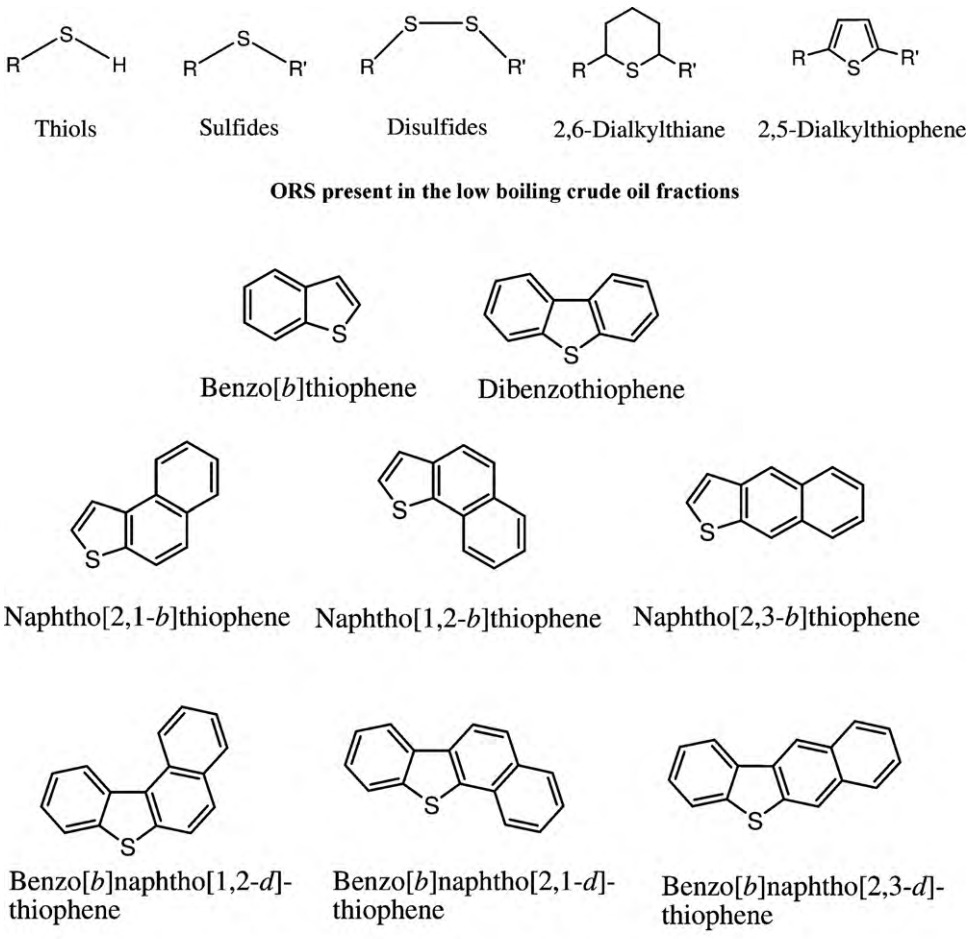

Fig. 1. ORS present in low and high boiling crude oil fractions.

low cost and valuable adsorptive characteristics [6–9]. The fundamental building units in natural zeolites are tetrahedral (TO_4) of four oxygen ions surrounding a central ion (T) of either Si^{4+} or Al^{3+} as a primary building unit (PBU) [10]. The linking together of PBU gives Secondary Building Unit (SBU), which is three-dimensional network in which each oxygen of a given tetrahedron is shared between this tetrahedron and one of four others [11]. The most common minerals in the Jordanian zeolite are phillipsite (Ph), faujasite, and chabazite (Ch) [7].

The important features of zeolites are high internal and external surface areas [12], chemical and mechanical stability [13,14], and layered structure [15]. Zeolites are excellent adsorbent materials [16]. The adsorption on zeolites can be described as physical adsorption [17].

The literature on adsorptive desulphurisation studies reveal rather a conflicting picture with many studies showing substantially lower capacities for the sulphur removal success with transportation fuels such as commercial diesel is far from being well understood. Further, a variety of the ORS has been studied for their removal and less attention has been paid to most important components such as benzothiophene (BT), dibenzothiophene (DBT), and 4,6-dimethyldibenzothiophene (DMDBT), which are critical from the point of view of diesel desulphurisation [18–21].

The main objective of this investigation is to study the physical characteristics of this adsorbent using various analytical methods such as Fourier transform infrared (FTIR), X-ray diffraction (XRD), X-ray fluorescence (XRF), and nitrogen adsorption/desorption isotherms. Furthermore, the capability of the ZT to adsorb the ORS will be ascertained. The study will also investigate the effect of key parameters such as particle size, initial total sulphur concentration, temperature on the adsorption process, and the nature of the mechanisms involved. In the second part of our work, a more detailed sulphur removal studies onto the ZT after various chemical modifications will be reported.

2. Materials and methods

2.1. Adsorbent

The materials used in this study were analytical grade reagents and were used as received without any further purification. The chemicals were purchased from the corresponding sources: cyclohexane (Fluka) and toluene (Pharmco). Commercial diesel fuel (density: 0.84 g ml^{-1}) was purchased from randomly selected private fuel stations in Amman. The ZT was collected from Tlul Al-Shahba by the natural resource authority (NRA)/Jordan. The diesel fuel samples of different ORS concentrations were prepared by sequential dilution of the commercial diesel fuel with n-heptane (Spectroscopic grade, Scharlau, density: 0.70 g ml^{-1}).

The ZT was ground and passed through different sieves in order to obtain samples with three particle sizes namely; (100–200),

(300–400), and (500–600) μm. The samples were washed with distilled water until become free from any fine particles. Then, they were dried in an oven at 105 °C for 48 h.

2.2. Mineralogical and chemical composition of the ZT's

The XRD spectra of the ZT and the ORS-loaded ZT (SLZT) samples were recorded using Shimadzu XRD-6000 Powder Diffractometer, operated at 30 kV and 30 mA, scatter slit: 1°, receiving slit: 0.3 mm, drive axis: 2θ, scan speed: 2°/min and sampling pitch: 0.02°. The diffraction patterns were identified by comparison with the standard patterns stored in the instrument library.

The chemical compositions of the ZT and the SLZT samples were also determined by the XRF method. The XRF measurements were carried out by a sequential wavelength dispersive X-ray fluorescence spectrometer (Shimadzu XRF–1800). The spectrometer was running at (60 kV, 140 mA), equipped with an X-ray tube of Rhodium anode. The loss on ignition (LOI) was determined after oxidising the sample at 950 °C. The major mineral oxides in the samples were determined on fused beads (glass discs) in which the samples material (0.70 g of the powdered sample) was diluted with 7.00 g of a flux agent (composed of 66% of di-Lithiumtetraborate and 34% of Lithiumborate). The fusion was carried out using a high frequency induction furnace (Claisee/Bis-Fuxer).

The FTIR analytical spectra were taken using a Shimadzu IR Prestige- 21/FTIR-8400S with a resolution of 4 cm^{-1} at 64 scans. Samples of particle size <66 μm were first dried at 110 °C for 24 h. The dried samples were mixed with finely divided KBr at a ratio of 1:300. Duplicate spectra were collected for the same sample. A previously recorded background spectrum was subtracted from the spectrum. All spectra were recorded from 4000 to 400 cm^{-1} and the spectra were collected using a Shimadzu IR Prestige-21 Windows Software.

Spent adsorbent samples were removed from the diesel after equilibration and were freed from the diesel by drying at 65 °C in preparation for the FTIR analysis. Small quantities of the adsorbent were ground with KBr and pressed by a provided tool.

2.3. Nitrogen adsorption studies

Nitrogen adsorption and desorption isotherms of the ZT were measured using Quantachrome® NovaWin2 instrument in order to calculate the surface area of the samples according to Brunauer–Emmett–Teller (BET) method. The surface areas of the studied ZT samples were automatically calculated by application of the BET equation [11].

2.4. Total ORS analysis

The ORS concentration in the diesel fuel samples was determined according to test method of American Standard Test Methods ASTM D4294 that covers the measurement of sulphur in hydrocarbons, such as diesel, naphtha, kerosene, residuals, etc. This test method is based on the energy-dispersive-X-ray fluorescence technique using Sulphur-In-Oil Analyser (HORIBA®).

The sample was placed in the beam emitted from an X-ray source with energy above 2.5 keV. The resultant excited characteristic X radiation was measured and the accumulated count was compared with counts from previously prepared calibration curve to obtain the sulphur concentration in mass% or ppmw. Moreover, the instrument was calibrated using three different standard sulphur concentrations: 0.1%, 0.5%, and 1.0% sulphur and a linear calibration curve was obtained.

2.5. Adsorption isotherms

A stock Jordanian diesel fuel, 9500 ppmw and the various concentrations composed of n-heptane were prepared and were used for all the ORS removal experiments. The ZT samples were sieved and the fractions with particle size ranges from 100 to 200, 300 to 400, and 500 to 600 μm were chosen for the adsorption measurements. To exactly 3.00 g of the ZT, 15.00 g (17.86 ml) sample of the diesel fuel was added in a 50 ml Erlenmeyer flask that was sealed well using a rubber stopper. Thirteen of such solutions were prepared and placed in a shaker (shaking water bath, GFL (Gesellschaft fur Lbortechnik mbH), 1083, Germany) at 25, 35, and 45 °C for 200 rpm. Enough shaking was performed to ensure a reasonably good relative movement between the ZT particles and the liquid. At predetermined times a sample was withdrawn and filtered on filter paper. Finally the filtrate was subjected to sulphur analysis by sulphur analyser. Six samples of the diesel fuel of different ORS concentrations; 500, 1000, 2000, 4000, 6000, and 8000 ppmw were also prepared and studied using three organic solvents namely; cyclohexane, n-heptane, and toluene.

2.6. Column experiments

The column experiments were carried out using vertical glass columns with 395 mm long and 22 mm inside diameter. One hundred gram of the ZT of each particle sizes was packed in the columns. About 2–3 g of sand glass was placed at the bottom of the column, to act as a filtration material for effluent sample. Diesel fuel with a 9500 ppmw initial ORS concentration was fed continuously by gravity on the top of the column in down flow mode at a fixed flow rate of 1 ml min^{-1} at 25 °C. The effluent sample was taken from the column continuously. Each 20 ml of the effluent sample was collected alone as portions and it was measured by the sulphur analyser to evaluate the concentration of the ORS in the samples.

Desorption studies were carried out for the loaded ZT samples using the same column that mentioned-above. A 10 ml of the n-heptane was used as a washing solvent (eluant). Each 10 ml was taken continuously from down flow of column at 25 °C, the ORS concentration was, then, measured.

3. Results and discussion

3.1. Mineralogical and chemical composition of the ZT's

The chemical compositions of the ZT and the SLZT were shown in Table 1.

As shown from Table 1, the content of SiO_2 is high for the ZT sample compared with Al_2O_3 as percentages 31.55% and 9.03%, respectively, which can be explained by the presence of quartz as indicated by the X-ray diffraction scans.

The percentages of the CaO, MgO, Na_2O, and K_2O for the ZT sample were 9.24%, 8.94%, 0.87%, and 1.38%, respectively. Therefore, the

Table 1
The chemical composition of the ZT and SLZT.

Constituent	ZT (wt%)	SLZT (wt%)
SiO_2	31.55	32.57
Al_2O_3	9.03	10.08
Fe_2O_3	13.94	12.04
Na_2O	0.87	2.25
MgO	8.94	5.57
CaO	9.24	5.97
K_2O	1.38	2.14
TiO_2	2.86	2.31
P_2O_5	0.66	0.53
LOI	14.63	–

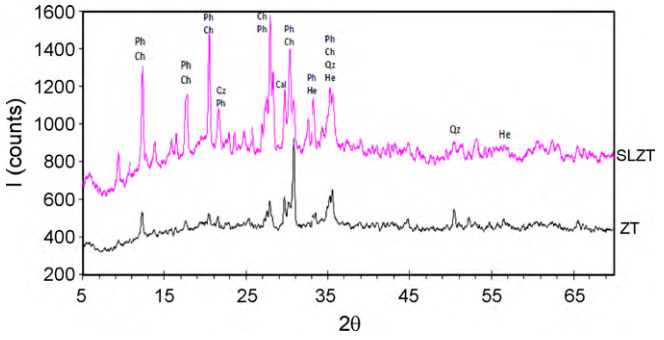

Fig. 2. The XRD patterns of the ZT and the SLZT.

type of natural zeolite founded in the ZT was Ca^{2+}, Mg^{2+}, Na^{+}, and K^{+} zeolite. The sodium and potassium cations in the zeolite might responsible for the adsorption of the ORS because the percentages of Na_2O and K_2O had been raised after adsorption of the ORS from 0.87% and 1.38% in the ZT to 2.25% and 2.14wt% in the SLZT; respectively. Besides, it can be seen that the percentages of the CaO and MgO had been lowered from 9.24% and 8.94% to 5.97% and 5.57%; respectively. It means that the exchangeable cations in the ZT are calcium and magnesium.

The XRD patterns comparison between the ZT and the SLZT are illustrated in Fig. 2. The ZT contains phillipsite (Ph) as the major natural zeolite constituent and chabazite (Ch) with a minor constituent. Quartz (Qz) was found to be the main constituent in addition to trace amount of hematite (He) and calcite (Cal). This figure shows the intensity of the peaks in the SLZT comparing with those in case of the ZT since the interactions between the ORS and the active sites on the ZT sample enlarged the 3-D mineral space as shown from d-spacing values presented in Table 2.

3.2. Surface and porous properties of the ZT

The N_2 adsorption/desorption isotherms of the ZT are shown in Fig. 3. According to IUPAC classification, it can be seen from Fig. 2 that the ZT sample shows a type III adsorption isotherm, meaning there is a wide range of pore sizes in the ZT. The shape of the adsorption isotherm curve itself represented a continuous progression with increasing loading from monolayer to multilayer adsorption and then to capillary condensation; indicating relatively weak attractive interactions between the adsorbent and the adsorbate [22].

On the other hand, the pore size distribution graph of the ZT sample is shown in Fig. 4. It was found that the most probable pores radii of the ZT were almost at: 18.75 Å and other probable maximums were seen around 24.07 and 35.84 Å. Therefore, the most pores radii were in range of micropores and some of these in range of mesopores. The average pore radius was 25.42 Å and the BET was 243.5 m^2/g.

Table 2
Representative XRD data of the ZT and the SLZT.

	ZT		SLZT	
Mineral (constituent)	2θSG	d-spacing (Å)	2θ	d-spacing (Å)
Ph	12.44	7.11	12.40	7.13
	28.27	3.16	27.48	3.24
Ch	9.55	9.26	9.42	9.37
	12.80	6.91	12.40	7.13
	30.93	2.89	30.43	2.94
	35.99	2.49	35.41	2.53
Qz	21.36	4.21	21.63	4.11

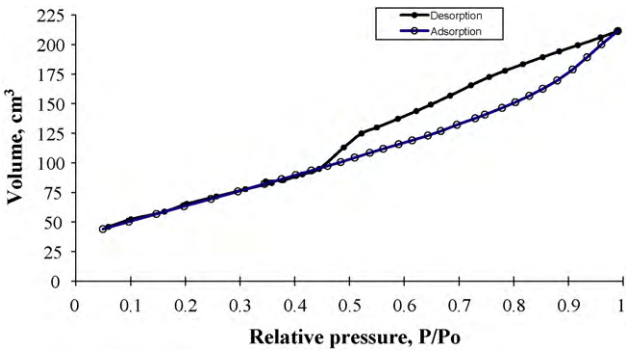

Fig. 3. The nitrogen adsorption/desorption isotherm of the ZT (A: adsorption, D: desorption).

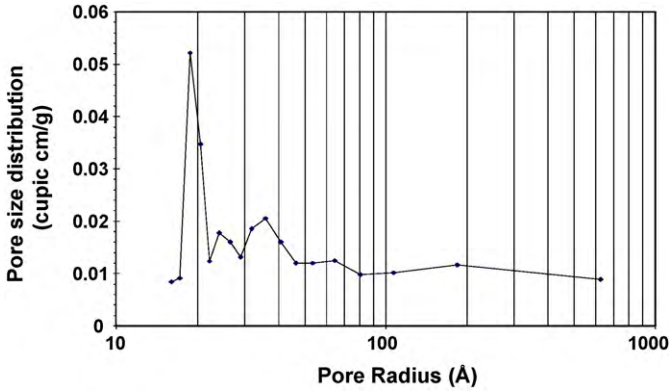

Fig. 4. The pore size distribution of ZT.

3.3. Adsorption isotherms

3.3.1. Effect of contact time

The effect of contact time on the ORS adsorption was investigated. The following contact times were chosen namely; 1.00, 4.00, 8.00, 12.00, 24.00, 36.00, and 48.00 h. The results of these experiments are shown in Fig. 5. It can be seen that the ORS adsorption onto the ZT for three particle size ranges was increased with increasing time and reached the maximum value after 8 h, and thereafter it remained constant (plateau). The removal of the ORS was occurred quickly and the shaking time of 8 h was enough to achieve the adsorption equilibration. At this equilibrium time of 8 h, the percent uptake of the 100–200, 300–400, and 500–600 μm were 8.09%, 7.08%, and 6.08%, respectively.

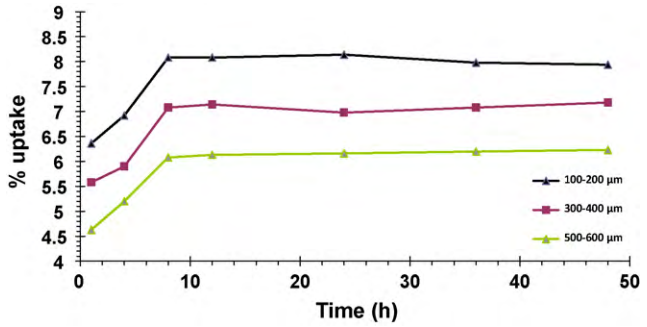

Fig. 5. Effect of contact time on the ORS adsorption onto the ZT. Experimental conditions: particle size: (100–200), (300–400), and (500–600) μm, temperature: 25 °C, time: 8 h, mass: 1 g and an initial ORS concentration of 5000 ppmw.

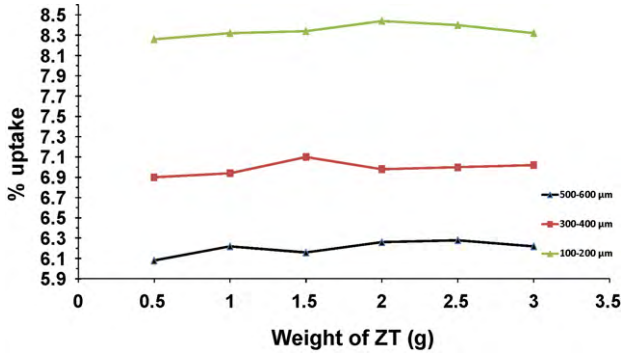

Fig. 6. Effect of the ZT mass on the ORS adsorption. Experimental conditions: particle size: (100–200), (300–400), and (500–600) μm, temperature: 25 °C, time: 8 h and an initial ORS concentration of 5000 ppmw.

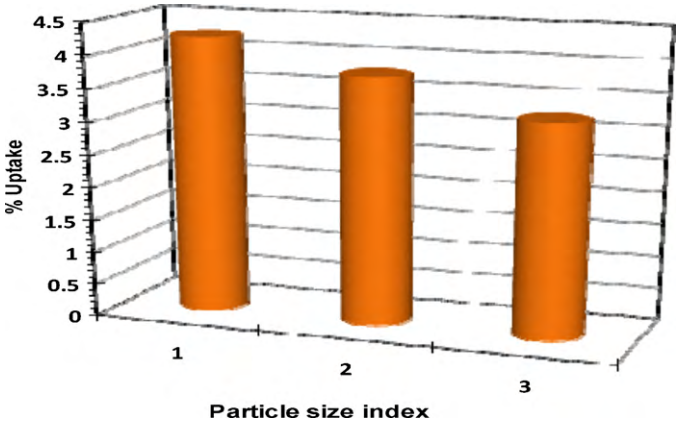

Fig. 7. Effect of the ZT particle size on the ORS adsorption. Experimental conditions: particle size: (100–200), (300–400), and (500–600) μm, temperature: 25 °C, time: 8 h, mass: 1 g and an initial ORS concentration of 9500 ppmw.

3.3.2. Effect of adsorbent mass

The effect of the ZT mass on the extent of the ORS removed was investigated. The following masses were used 0.50, 1.00, 1.50, 2.00, 2.50, and 3.00 g and the results are shown in Fig. 6. It is clear from Fig. 6 that there are no significant variances in sulphur uptake when different masses of ZT were used. This could be explained by that the mass of the ZT to the unit surface area available for the ORS adsorption was identical. Hence, the weight of ZT of 1 g was chosen.

3.3.3. Effect of particle size

The effect of the particles size on the adsorption process is shown in Fig. 7. It is clear from Fig. 7 that there is a little effect for the particle size on the adsorption process. This behaviour indicated that the mechanism of the ORS adsorption onto the ZT did not depend only on the particle size (i.e. surface area or channels). Therefore, the best adsorption was observed using the particle size range of 100–200 μm.

3.3.4. Effect of temperature

Fig. 8 shows that the ORS uptake by the ZT for the three particle size ranges is decreased as the temperature increases which implies an exothermic process. The adsorption isotherm at 25 °C showed the highest adsorption capacity (Q) values over the three temperatures studied. Therefore, it is more desirable to carry out the adsorption reaction at 25 °C which is the closest to the normal room temperature.

3.3.5. Effect of solvent

The effect of solvent on the adsorption processes is shown in Fig. 9. It can be observed that the ORS uptake by the ZT was decreased as using the aromatic solvent because the thiophene compounds which are principal ORS compounds in the diesel fuel would have a great affinity toward aromatic compound such as benzene or toluene due to the fact that both are similar species and, as a result, would compete against the zeolite adsorbents for interactions [23]. The adsorption isotherms using cyclohexane or n-heptane showed the highest Q values over the studied initial concentration range. However, n-heptane is present in large quantities in commercial premises with low price analogised with cyclohexane that has a high price. For that, it was more desirable to carry the batch experiments by employing n-heptane as a solvent for diluting the diesel fuel samples.

3.3.6. The Langmuir and Freundlich adsorption isotherms

The adsorption isotherms were analysed using linearised Langmuir and Freundlich equations. The results are shown in Fig. 10.

Fig. 10 shows the adsorption isotherm curves for the ORS adsorption onto the ZT. The L-shaped adsorption isotherms were obtained for the samples which indicated a decreasing slope as concentration increased, suggesting the adsorbent has a high affinity for the adsorptive at low concentration, but as the concentration increased, the affinity of the adsorptive decreased because empty adsorbent sites were preoccupied.

It can also be observed that the Langmuir and the Freundlich equations can be used to describe the adsorption data. However, the Freundlich adsorption model have a better correlation coefficient than the Langmuir equation as was evidenced from R^2 values that it assumes unlimited adsorption sites which correlated with a heterogeneous surfaces of the ZT [24,25].

The Langmuir isotherm model would be used to estimate the adsorption capacity, Q and K_L as presented in Table 3. The data of Q exhibited that the ZT were ordered as a stronger of the ORS adsorption by the following: 100–200 > 300–400 > 500–600 μm. This could be attributed to the higher surface area and the larger average pore volume of the smaller particle size. On the one hand, the data of the K_L indicated that the ZT are order as a stronger of the affinity of the adsorbate (ORS) to the adsorbent (ZT) by the following: 100–200 > 300–400 > 500–600 μm.

On the basis of the Freundlich isotherm, a relatively slight slope (the figure not shown here) (and hence a high value of n) indicated that the adsorption is good over the entire range of concentrations studied, while a steep slope (and hence small n) means that the adsorption is good at high concentrations but much less at lower concentrations [26]. In other words, a greater value of the intercept K_F indicates a higher capacity for adsorption than a smaller value

Table 3
The Freundlich and the Langmuir adsorption isotherm parameters for the adsorption of the ORS onto the ZT at 25 °C.

Particle size (μm)	Langmuir isotherm			Freundlich isotherm			
	R^2	K_L (dm^3/g)	Q (mg/g)	R^2	n	$1/n$	K_F (mg/g)(mg/dm^3)
100–200	0.8971	7.55×10^{-3}	7.15	0.9459	8.052	0.124	2.44
300–400	0.9261	5.04×10^{-3}	6.32	0.9524	6.558	0.153	1.67
500–600	0.9178	3.34×10^{-3}	5.52	0.9442	5.171	0.193	1.01

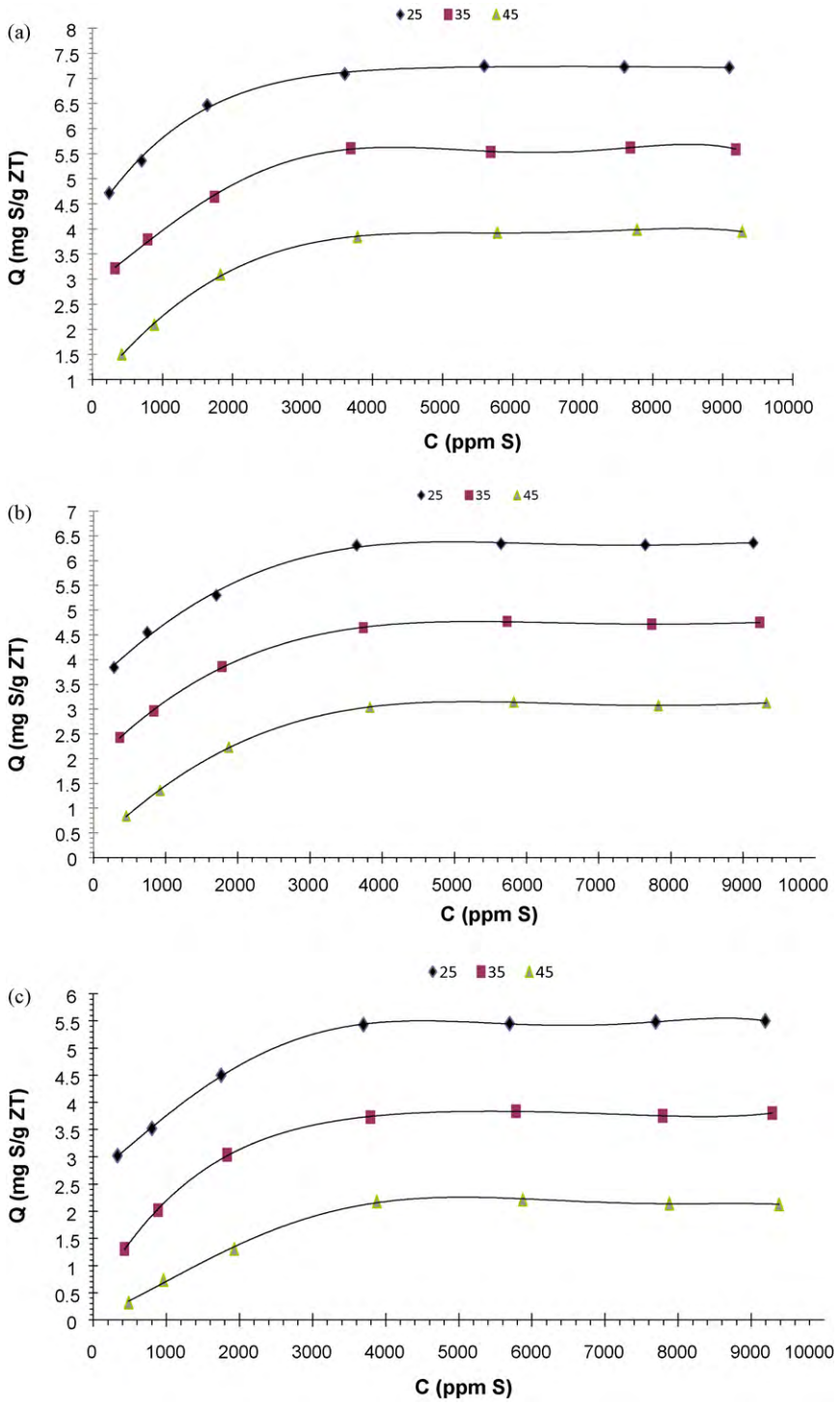

Fig. 8. The ORS adsorption isotherms onto the ZT with different bath temperatures at 25 °C, 35 °C, and 45 °C for different particle sizes (a: (100–200), b: (300–400), c:(500–600) μm).

Table 4
Adsorption capacities of the ORS adsorption onto various adsorbents..

Adsorbent	Adsorption capacity (mg/g)	References
Ni on silica	1.7	[27]
Cu on zirconium	15.7	[28]
CoMo on active carbons	17.0–34.6	[29]
Carbon aerogels	15.1	[24]
Ni and Cu on Y-zeolites	31.0–42.0	[30]
Y-zeolites with Cu, Ni, Zn, Pd, and Ce ions	4.5–10.0	[31]
Treated and acid activated bentonite	2.46–4.79	[32]

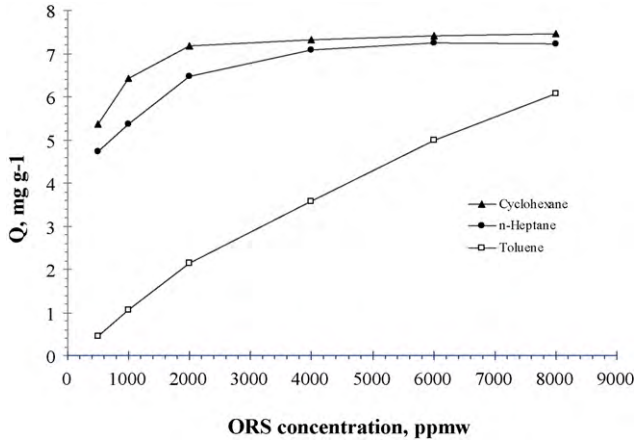

Fig. 9. Effect of solvent on the ORS adsorption. Experimental conditions: particle size: (100–200) μm, temperature: 25 °C, time: 8 h and mass: 1 g.

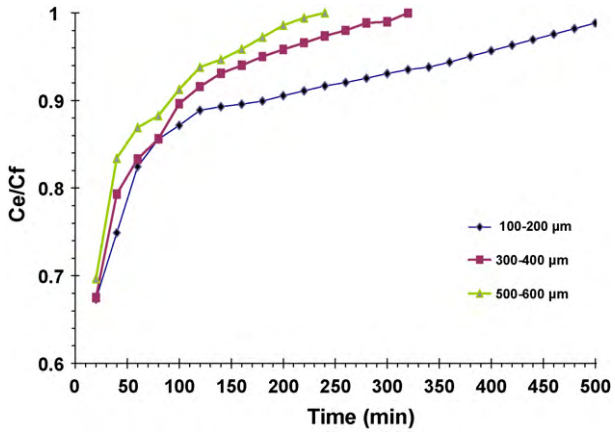

Fig. 11. Breakthrough curve of the ORS adsorption onto the ZT using three particle size ranges of 100–200 μm, 300–400 μm, and 500–600 μm at constant feed concentration of 9500 ppmw.

[26]. It can be seen from Table 3 that the n values corresponded to the ZT were ordered as a larger in n values and K_F by following: 100–200 > 300–400 > 500–600 μm. The numerical value of $1/n < 1$ for three ranges of the ZT indicated that the adsorption capacity was only slightly suppressed at lower equilibrium concentration. However, Table 4 summaries the adsorption capacities of the adsorption of ORS onto various adsorbents.

3.4. Column experiments

The results of the column adsorption studies are shown in Fig. 11. It can be remarked that the ORS uptake by the three ranges of the ZT was decreased as time of taken effluent sample increased because the ORS that adsorbed was filled the most of active sites on the surface of the ZT. The breakthrough curve were plotted giving ratio of effluent to the feed concentrations (C_e/C_f) and time (min) for varying particle size ranges of the ZT, where C_e is the effluent concentration and C_f is the feed concentrations.

The column capacity (Q_c) was calculated using Eq. (1) [33]. The Q_c values were: 4.45, 2.57, and 1.92 mg/g for 100–200, 300–400, and 500–600 μm, respectively. The values of the adsorption capacities in this experiment were quite smaller than those obtained in batch experiments; this result was expected since there was no mechanical shaking of the sample as in the batch experiments. However, the ORS adsorption depended on the flow rate and the distribution of the ZT particles [34].

$$Q_c = \frac{\text{ORS adsorbed on adsorbent bed (mg)}}{\text{mass of adsorbent in bed (g)}} \quad (1)$$

The breakthrough curves for the ZT with three particle size ranges of 100–200, 300–400, and 500–600 μm, indicated that the concentration of the ORS in the effluent become close to the feed concentration at 540, 320, and 240 ml, respectively, this means that the efficiency of columns decreased when used large range of particle size of the ZT. On the other hand, if the feed concentration increases then loading rate increases, and the adsorption capacity increases [33]. For this reason, in present column experiments, the feed concentration was 9500 ppmw which was the largest ORS concentration of the diesel sample in this study.

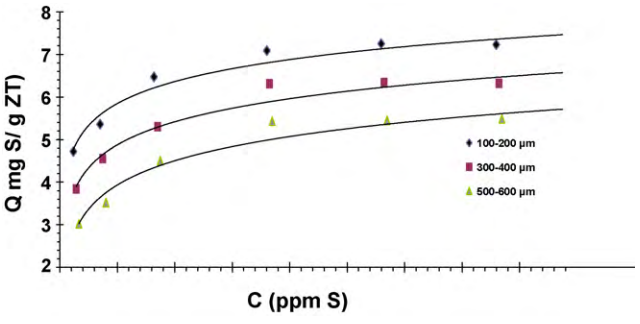

Fig. 10. Adsorption isotherms of the ZT with various particle size ranges of 100–200 μm, 300–400 μm, and 500–600 μm.

3.4.1. Column regeneration

Plots of the effluent ORS concentration versus the bed volume (n-heptane flow through the column) are shown in Fig. 12 and Table 5.

It can be observed that the ORS concentration of the effluent samples decreased as going from the first to the last portion. Furthermore, this phenomenon depended on efficiency of n-heptane to remove the ORS from the ZT surface and its pores. Stepan [14] showed that no adsorbent deactivation was found in column after washing of the adsorbent with n-heptane followed by drying at 100 °C that is sufficient for the complete adsorbent regeneration.

It can be seen that the high recovery was observed for the largest one of the particle size range (500–600 μm). Since the high loading of the ORS on the active sites is confirmed when using the smaller particle size of the ZT, more numbers of the ORS molecules would be retained, and, therefore, the percentage of the ORS recovery would not be completed.

3.4.2. Mechanisms of adsorption

Understanding the mechanism of ORS adsorption on solid oxide surfaces is essential for the removal of the ORS from liquid fuel [35]. The ORS present in the diesel fuel are of varying chemical and physical properties and as a result, interact differently with various types of adsorbents. The driving force for adsorption results from: (i) specific character of the solute relative to the particular solvent (i.e. solubility) and (ii) a specific affinity of the solute for the solid. This kind of attraction may be predominantly one of electrical, van der Waals, or of a chemical nature. Consequently, the surface chemistry of the adsorbents and its effect on the adsorption process was investigated in order to interpret the ORS adsorption results on various adsorbents.

The FTIR technique is an interesting application for studying the interaction between an adsorbate and the active groups on the surface of the adsorbent. Parameters like particle size and temperature play very important roles in determining the adsorption mechanism [35]. A systematic approach relating the ORS adsorption performance of the ZT to their surface chemistry was investigated.

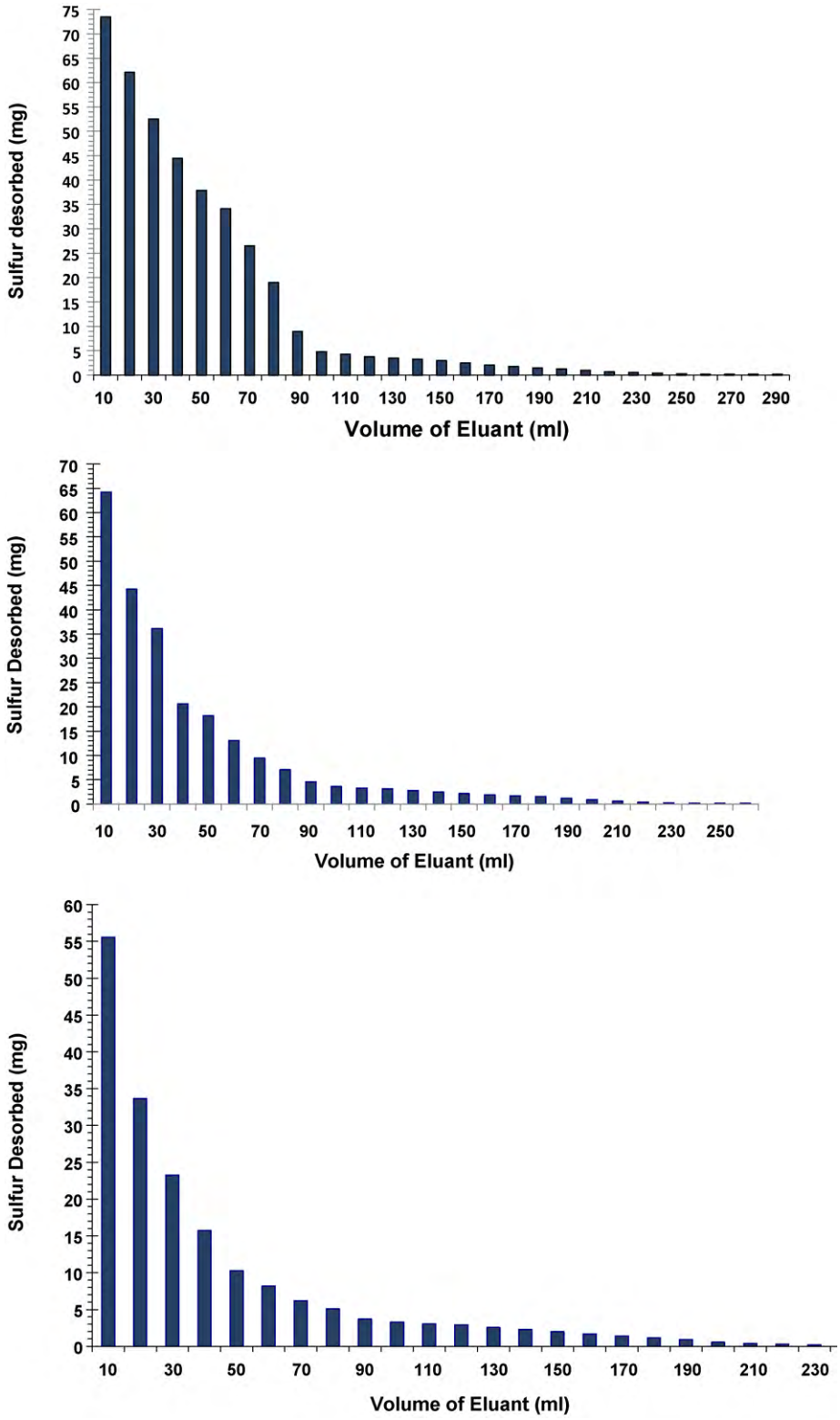

Fig. 12. Effect of the particle size ranges on the column regeneration.

Table 5
The percentage recovery (wt%) of the ZT at different particle size ranges using n-heptane.

Particle size (μm)	Total adsorbed (mg)	Total desorbed (mg)	Total retained (mg)	Percentage recovery (wt%)
100–200	445.0	391.4	53.6	88.0
300–400	257.2	243.8	13.4	94.8
500–600	191.7	184.4	7.3	96.2

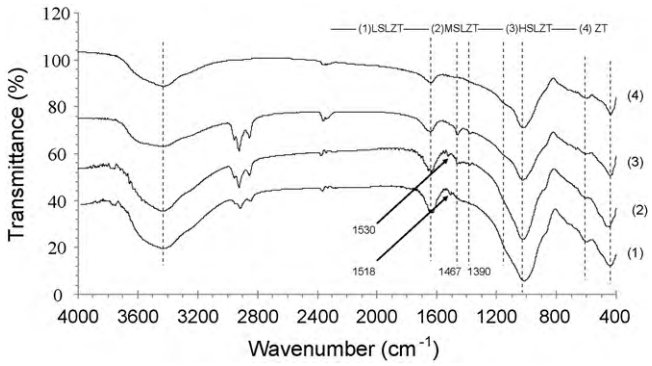

Fig. 13. FTIR spectra of ZT, LSLZT, MSLZT, and HSLZT.

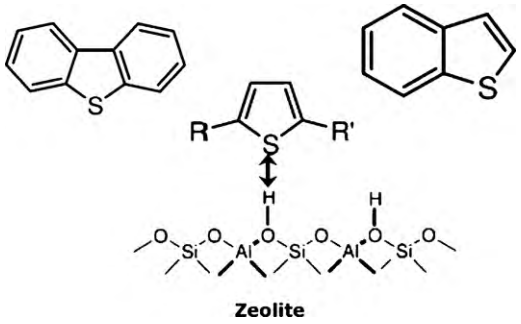

Scheme 1. Thiophene interaction with Brønsted site of the ZT through S atoms.

Fig. 13 shows the FTIR spectra for the ZT. The bands in the region 3480–3750 cm^{-1} can be assigned to O–H vibration [36,7]. The band at 3565 and 3485 cm^{-1} were due to hydrogen bonded Si(Al)OH. The bonded water absorption broad bands were found at 3448, 3287, and 3203 cm^{-1}, which indicated the different types of bonding and location for the water molecules. Thus, the high frequency band at 3448 cm^{-1} could be attributed to trapped water within the ZT structure and the bending vibration of H_2O was found at 1650 cm^{-1}. The spectrum clearly showed the three characteristic zeolitic spectral bands, those arising from asymmetric stretching vibrations, which appear as strong band at 1018 cm^{-1} due to Ph and Ch, and a peak at 1141 cm^{-1} due to the latter two zeolites; symmetric stretching vibrations at 772 cm^{-1} for Ch, and 670 cm^{-1} for Ph; and the bending vibrations which appear at 444 cm^{-1} for Ph [37,7].

The FTIR spectrum (not shown here) for the diesel fuel exhibited characteristic absorption bands for the major functional groups involved in the aliphatic alkyl chains. The absorption band around 720 cm^{-1} indicated $[-CH_2-]_n$ rocking of the methylene groups. The absorption bands in the regions 2950–2750 cm^{-1} were assigned to (–CH, $-CH_2$ and $-CH_3$) carbon–hydrogen stretching vibrations of the aliphatic alkyl chains [12]. It also showed that the absorption bands of the bending vibrations around 1460 cm^{-1} which were indicative of the ($-CH_2$ and $-CH_3$) groups while those at 1380 cm^{-1} were indicative of the ($-CH_3$) groups [38].

Shifts or changes of these peaks would indicate interactions of the ORS with the functional groups onto the ZT surface, and can be interpreted as adsorption on neutral sites (Table 6). Four samples of the ZT were selected for FTIR analysis namely; raw ZT and loaded ZT with different ORS concentrations; 500, 4000, and 9500 ppmw and the results are also shown in Fig. 13. It showed a quite different absorption patterns. In contrast to the ZT, strong absorption band were observed at 1660, 2880, 2930, and 2970 cm^{-1} which were assigned to the presence of the ORS on the surface of the ZT; incremented from low (LSLZT), medium (MSLZT) to high (HSLZT) ORS-loaded on the ZT.

As it is shown from Fig. 13, a slight shift and change is observed for the 3448 and 920 cm^{-1} bands. This would be attributed to interaction of the ORS onto the O–H groups of the ZT. New peaks were also detected at 1390, 1463, and 2929 cm^{-1}. These changes could be attributed to the involving of the O–H groups in the adsorption of the ORS from diesel fuel and different adsorption modes of thiophene.

The FTIR band at 1463 cm^{-1} was observed, and it was ascribed to a shift of $\nu(C{=}C)_{sym}$ to higher frequencies. The shift of $\nu(C{=}C)_{sym}$ to the higher frequencies was caused by the increased electron density within the C=C–C=C fragment when thiophene was coordinated via a S atom [16]. Analogously, the two new bands at 1436 and 1390 cm^{-1} were tentatively ascribed to the $\nu(C{=}C)_{sym}$ of thiophene adsorbed onto the ZT via S atom. The bands at 1530 or 1518 cm^{-1} due to the asymmetric stretching vibration of C=C of thiophene was more evident on the LSLZT and MSLZT than on HSLZT. The enhanced intensity of the 1530 or 1518 cm^{-1} bands for thiophene adsorbed onto LSLZT and MSLZT could be regarded as evidence that the adsorbed thiophene molecules interact with the ZT by S atoms, and consequently result in the increase of the dipole moment of C=C. Therefore, it can be deduced from the Fig. 13 that there are two modes of the thiophene adsorption onto the ZT. One is that the parallel adsorption of the thiophene molecule onto the surface of the ZT; the other is that the thiophene adsorption with the Brønsted site of the ZT through S atoms (Scheme 1).

Here, it would be expected that all ORS (aliphatic and aromatic) participate in the adsorption process. This phenomenon was supported by the formation of new peaks when the high ORS (HSLZT sample) was used in the adsorption. While, only aromatic ORS were participated in the adsorption process when the low ORS concentration was used. In fact, the appearance of the new peaks could be attributed to: (a) the accumulation of the ORS onto the ZT surface as a result of the polar S–C bond stretching and bending, (b) the ORS adsorption by the ZT groups that may affect their strength and hence created new types of absorptions bands, and (c) the π–n interactions that might be developed between the cyclic ORS and the ZT.

During the batch adsorption experiments, a little gas was evolved. This gas might be H_2S forms via C–S bond cleavage in the thiophene-derived carbocations to form unsaturated fragments on Brønsted acid sites [1] (Scheme 2). The results revealed that the aromatics present in the diesel fuel strongly competed with the ORS for the available adsorption active sites. Diesel fuel typically contains

Table 6
Assignment of IR bands in ZT spectrum.

Frequency (cm^{-1})	Band assignment (ZT)	Frequency (cm^{-1}) (after adsorption)		
		HSLZT	MSLZT	LSLZT
3433	Symmetric stretching for OH from water bounded by H bridges	3439	3441	3433
1639	Bending for H–OH	1645	1639	1637
1141	Asymmetric stretching for external tetrahedral linkages	Disappear	Disappear	Disappear
1020	Stretching asymmetric for internal tetrahedral	1026	1024	1014
600	Symmetric stretching for internal tetrahedral	605	605	598
440	Bending for internal tetrahedral	442	447	444

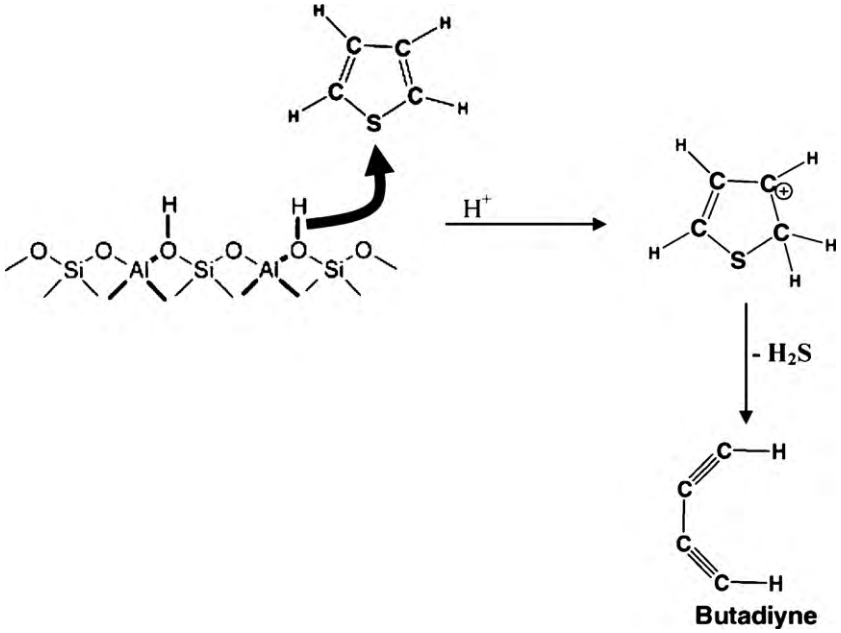

Scheme 2. Thiophene ring opening reaction and formation of H_2S and C4 fragments.

a considerable amount of aromatics in addition to relatively small amounts of refractory sulphur containing compounds [1]. Thus, in the adsorption process, a likely tough and mandatory competition between the aromatics and the ORS for the active sites would detriment the adsorbent capacity and the selectivity as well. In such a competitive environment, the adsorbent identity definitely would play a role in this respect.

The first process may take place near the exterior surface of the ZT particles and the external aluminium silicates groups were also participate in the adsorption. The second process may take place in the ZT layers and results in a uniform distribution of adsorbed ORS.

4. Conclusion

The ZT is predominantly composed of mainly phillipsite and Chabazite, in addition to a considerable amount of quartz and trace amount of hematite and calcite. There is a little effect for the particle size on the adsorption process. This behaviour indicated that the mechanism of the ORS adsorption onto the ZT did not depend only on the particle size (i.e. surface area or channels). The effect of the operating parameters such as the initial ORS concentration, the bath temperature, contact time, and the solvents type on the ORS adsorption was investigated and the optimised conditions were applied. The adsorption capacities were decreased as the temperature increased as the type of the adsorption was exothermic. The regeneration efficiency of the spent ZT in the column experiment was 81.5%.

The adsorption capacities of the ZT were not only comparable to other related adsorbents but also were better than some commercial adsorbents, such as treated and acid activated bentonite and on silica supported by Ni. Consequently, the Jordanian ZT still has the advantage of its low cost comparing with common commercial adsorbents. Overall, the ORS adsorption using the Jordanian ZT from a diesel fuel of a high ORS content, like the Jordanian diesel fuel, could be used as a complementary or primary desulphurisation process in order to reduce the huge cost accompanied by the traditional or deep HDS process.

References

[1] A. Chica, K. Strohmaier, Iglesia, Effects of zeolite structure and aluminium content on thiophene adsorption, desorption, and surface reactions, Appl. Catal. B 60 (2005) 231–240.
[2] D. Stirling, The Sulfur Problem: Cleaning up Industrial Feedstocks, The Royal Society of Chemistry, Cambridge CB4 OWF, UK, 2000.
[3] J.G. Speight, The Desulfurization of Heavy Oils and Residua, 2nd ed., Marcel Dekker, Inc., 1999.
[4] A.A. Yahia, S.B. Hisham, Sulfur removal from model diesel fuel using granular AC from dates' stones activated by $ZnCl_2$, Fuel 88 (2009) 87–94.
[5] M.B. Vinay, H.K. Chang, G.P. Jung, H. Sang-Sup, C. Soon-Haeng, K. Jong-Nam, Desulfurization of diesel using ion-exchanged zeolites, Chem. Eng. Sci. 61 (2006) 2599–2608.
[6] I. Dwairi, Jordanian zeolites evaluation for possible inclustrial application of natural aritain phillipsite tuff, Dirasat 19 (1992) 23–43.
[7] R. Yousef, M. Tutunji, G. Derwish, S. Musleh, Chemical and structural properties of jordanian zeolitic tuffs and their admixtures with urea and thiourea: potential scavengers for phenolics in aqueous medium, J. Colloid Interface Sci. 216 (1999) 348–359.
[8] M. Davila-Jimenez, M. Elizalde-Gonzalez, J. Mattusch, P. Morgenstern, M.A. Perez-Cruz, Y. Reyes-Ortega, R. Wennrich, H. Yee-Madeira, In situ and ex situ study of the enhanced modification with iron of clinoptilolite-rich zeolitic tuff for arsenic sorption from aqueous solutions, J. Colloid Interface Sci. 322 (2008) 527–536.
[9] M. Al-Anber, Z. Al-Anber, Utilization of natural zeolite as ion-exchange and sorbent material in the removal of iron, Desalination 225 (2008) 70–81.
[10] L. Mccusker, F. Liebau, G. Engelhardt, Nomenclature of structural and compositional characteristics of ordered microporous and mesoporous materials with inorganic hosts, Pure Appl. Chem. 73 (2001) 381–394.
[11] R. Barrer, Zeolites and Clay Minerals as Sorbents and Molecular Sieves, 1st ed., Academic press Inc., London & New York, 1978.
[12] M. Jiang, F. Ng, Adsorption of benzothiophene on Y zeolites investigated by infrared spectroscopy and flow calorimetry, Catalysis Today 116 (2006) 530–536.
[13] V. Radak, I. Gal, R. Radulović-Hercigonja, D. Seidel, Some physical and chemical properties of Fe(II)X, Fe(II)Y and Fe(III)Y zeolites, J. Inorg. Nucl. Chem. 40 (1978) 75–77.
[14] R. Stepan, Selective adsorption of sulfur compounds from hydrocarbon mixtures, Unpublished Doctoral Dissertation, University of Western Ontario, London, Ontario, 1999.
[15] B. Wang, Zeolite deactivation during hydrocarbon reactions: characterisation of coke precursors and acidity, product distribution, A Thesis submitted for the degree of Doctor of Philosophy of the University College London, United Kingdom, 2007.
[16] F. Tian, W. Wu, Z. Jiang, C. Liang, Y. Yang, P. Ying, X. Sun, T. Li, C. Cai, The study of thiophene adsorption onto La(III)-exchanged zeolite NaY by FT-IR spectroscopy, J. Colloid Interface Sci. 301 (2006) 395–401.
[17] A. Demirbas, Adsorption of sulfur dioxide from coal combustion gases on natural zeolite, Energy Sources 28 (2006) 1329–1335.

[18] B. Chen, N. Goh, L. Chia, Determination of copper by zeolite molecular sieve modified electrode, Electrochim. Acta 42 (1997) 595–604.
[19] A. Englert, J. Rubio, Characterization and environmental application of a Chilean natural zeolite, Int. J. Miner. Process. 75 (2005) 21–29.
[20] J. Cui, X. Zhang, H. Liu, S. Liu, K. Yeung, Preparation and application of zeolite/ceramic microfiltration membranes for treatment of oil contaminated water, J. Membr. Sci. 325 (2008) 420–426.
[21] M. Stylianou, V. Inglezakis, K. Moustakas, S. Malamis, M. Loizidou, Removal of Cu(II) in fixed bed and batch reactors using natural zeolite and exfoliated vermiculite as adsorbents, Desalination 215 (2007) 133–142.
[22] S. Lowell, E. Joan, A. Martin, Characterization of Porous Solids and Powders: Surface Area, Pore Size, and Density, Kluwer Academic Publishers, The Netherlands, 2004.
[23] A. Maldonado, R. Yang, Desulfurization of liquid fuels by adsorption via π complexation with Cu(I)–Y and Ag–Y zeolites, Ind. Eng. Chem. Res. 42 (2003) 123–129.
[24] S. Haji, C. Erkey, Removal of dibenzothiophene from model diesel by adsorption on carbon aerogels for fuel cell applications, Ind. Eng. Chem. Res. 42 (2003) 6933–6937.
[25] G. Limousin, J. Gaudet, L. Charlet, S. Szenknect, V. Barthe's, M. Krimissa, Sorption isotherms: a review on physical bases, modeling and measurement, Appl. Geochem. 22 (2007) 249–275.
[26] R. Donate, A. Akdogan, E. Erdem, H. Ceti, Thermodynamics of Pb^{2+} and Ni^{2+} adsorption onto natural bentonite from aqueous solutions, J. Colloid Interface Sci. 286 (2005) 4–52.
[27] J. Park, C. Ko, K. Yi, J. Park, S. Han, S. Cho, J. Kim, Reactive adsorption of sulfur compounds in diesel on nickel supported on mesoporous silica, Appl. Catal. B 81 (2008) 244–250.
[28] P. Baeza, G. Aguila, F. Gracia, P. Araya, Desulfurization by adsorption with copper supported on zirconia, Catalysis Communications, in press.
[29] H. Farag, Selective adsorption of refractory sulfur species on active carbons and carbon based CoMo catalyst, J. Colloid Interface Sci. 307 (2007) 1–8.
[30] V. Bhandari, C. Ko, J. Park, S. Han, S. Cho, J. Kim, Desulfurization of diesel using ion-exchanged zeolites, Chem. Eng. Sci. 61 (2006) 2599–2608.
[31] S. Velu, X. Ma, C. Song, Selective adsorption for removing sulfur from jet fuel over zeolite-based adsorbents, Ind. Eng. Chem. Res. 42 (2003) 5293–5304.
[32] M. Sultan, Adsorption of sulfur compounds in jordanian diesel fuel by jordanian bentonite, Unpublished Master's Thesis, University of Jordan, Amman, Jordan, 2009.
[33] J. Goel, K. Kadirvelu, C. Rajagopal, V.K. Garg, Removal of lead (II) by adsorption using treated granular activated carbon: batch and column studies, J. Hazard. Mater. B125 (2005) 211–220.
[34] E. Guibal, Interactions of metal ions with chitosan-based sorbents: a review, Sep. Purif. Technol. 38 (2004) 43–74.
[35] M.A. Al-Ghouti, M.A.M. Khraisheh, S.J. Allen, M.N. Ahmad, The removal of dyes from textile wastewater: a study of the physical characteristics and adsorption mechanisms of diatomaceous earth, J. Environ. Manage. 69 (2003) 229–238.
[36] G. Christidis, D. Moraetisa, E. Keheyanb, L. Akhalbedashvilic, N. Kekelidzec, R. Gevorkyand, H. Yeritsyane, H. Sargsyan, Chemical and thermal modification of natural HEU-type zeolitic materials from Armenia, Georgia and Greece, Appl. Clay Sci. 24 (2003) 79–91.
[37] Y. Nong, Y. Chun, X. Jian, F. Peng, C. Hong, An empiric linear formula between the internal tetrahedron symmetric stretch frequency and the Al content in the framework of KL molecular sieves, Chin. Chem. Lett. 14 (2003) 870–873.
[38] O. Bashir, Assessment of used vegetable oils blended with jordanian diesel as bio-diesel fuel, Unpublished Master's Thesis, University of Jordan, Amman, Jordan, 2008.